Journal of Medicinal Chemistry

Article

Cite This: J. Med. Chem. 2019, 62, 4979−4990

pubs.acs.org/jmc

Pharmacokinetics-Driven Optimization of 4(3*H*)-Pyrimidinones as Phosphodiesterase Type 5 Inhibitors Leading to TPN171, a Clinical Candidate for the Treatment of Pulmonary Arterial Hypertension

Zhen Wang,[†,#] Xiangrui Jiang,[†,#] Xianglei Zhang,[†,‡,#] Guanghui Tian,[§] Rulei Yang,[§] Jianzhong Wu,[§] Xiaoli Zou,[§] Zheng Liu,[∥] Xiaojun Yang,[∥] Chunhui Wu,[∥] Jing Shi,[∥] Jianfeng Li,[†] Jin Suo,[†] Yu Wang,[†] Rongxia Zhang,[†] Zhijian Xu,[†] Xudong Gong,[†,⊥] Yang He,[†] Weiliang Zhu,[†,‡] Haji Akber Aisa,[⊥] Hualiang Jiang,[*,†,‡] Yechun Xu,[*,†,‡] and Jingshan Shen[*,†,‡]

[†]CAS Key Laboratory of Receptor Research, Drug Discovery and Design Center, Shanghai Institute of Materia Medica, Chinese Academy of Sciences, Shanghai 201203, China

[‡]School of Pharmacy, University of Chinese Academy of Sciences, Beijing 100049, China

[§]Vigonvita Life Science Co., Ltd., Suzhou 215123, China

[∥]Topharman Shanghai Co., Ltd., Shanghai 201203, China

[⊥]Key Laboratory of Plant Resources and Chemistry in Arid Regions, Xinjiang Technical Institute of Physics and Chemistry, Chinese Academy of Sciences, Urumqi 830011, China

Supporting Information

ABSTRACT: Phosphodiesterase type 5 (PDE5) inhibitors are first-line therapy for pulmonary arterial hypertension (PAH) and erectile dysfunction. As a continuing work to improve the terminal half-lives and oral bioavailabilities of our previously reported 4(3*H*)-pyrimidones, a pharmacokinetics-driven optimization focusing on the terminal substituent is described. Two major congeneric series of 4(3*H*)-pyrimidones, the aminosulfonylphenylpyrimidones and acylaminophenylpyrimidones, were designed, synthesized, and pharmacologically assessed in vitro and in vivo. Among them, compound **15** (TPN171) with subnanomolar potency for PDE5 and good selectivity over PDE6 was finally recognized as a potential drug candidate, and its pharmacokinetic profiles in rats and dogs are significantly improved compared to the starting compound (**3**). Moreover, TPN171 was proven to exert a longer lasting effect than sildenafil in animal models, providing a foundation for a once-daily oral administration for its clinical use. TPN171 is currently being investigated in a phase II clinical trial for the treatment of PAH.

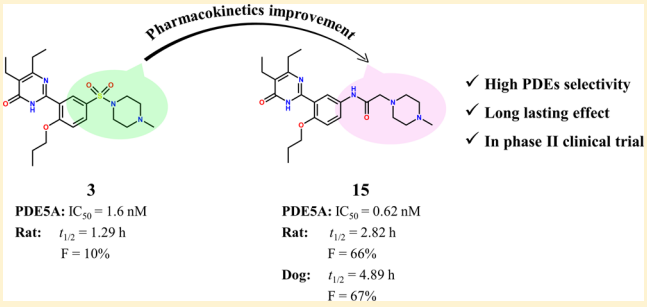

INTRODUCTION

Pulmonary arterial hypertension (PAH) is a progressive disorder characterized by abnormally high blood pressure in the pulmonary artery that carries blood from the heart to the lungs, ultimately leading to right heart failure and death.[1−4] It is a rare disease with a high mortality rate. Although survival of PAH patients is still unsatisfactory and annual mortality from this devastating disease remains high (∼10% per year), the therapy for PAH has evolved progressively in the past decade.[5,6] Several effective drugs, including cyclic nucleotide phosphodiesterase-5 (PDE5) inhibitors, a soluble guanylate cyclase stimulator, prostacyclin receptor agonists, and endothelin receptor antagonists, have been approved.[7−11] For instance, sildenafil and tadalafil, two inhibitors of PDE5 responsible for specifically cleaving cyclic guanosine monophosphate (cGMP), have been approved by the FDA for the treatment of PAH.[12−14] The pulmonary vasculature contains substantial amounts of PDE5, and regulation of NO/cGMP signaling cascades by inhibition of this enzyme results in a decrease of the pulmonary pressure due to vasodilation of the pulmonary artery.[15] PDE5 inhibitors also exert antiproliferative effects on pulmonary artery smooth muscle cells.[16] These features make PDE5 inhibitors advantageous for the treatment of PAH.[17−19] In addition, PDE5 inhibitor administration is not only taken as a monotherapy but is also used in combination with other drugs such as the endothelin receptor antagonist to improve long-term outcomes in PAH.[20]

We previously described the discovery of a series of 4(3*H*)-pyrimidinones as novel, potent, and selective inhibitors of PDE5 for potential use in PAH as well as male erectile dysfunction (ED).[21−23] The 11 subfamilies of human PDEs (PDE1−11) possess a conserved C-terminal catalytic domain for hydrolysis of the ubiquitous second messenger, cyclic

Received: January 21, 2019
Published: April 25, 2019

DOI: 10.1021/acs.jmedchem.9b00123
J. Med. Chem. 2019, 62, 4979−4990

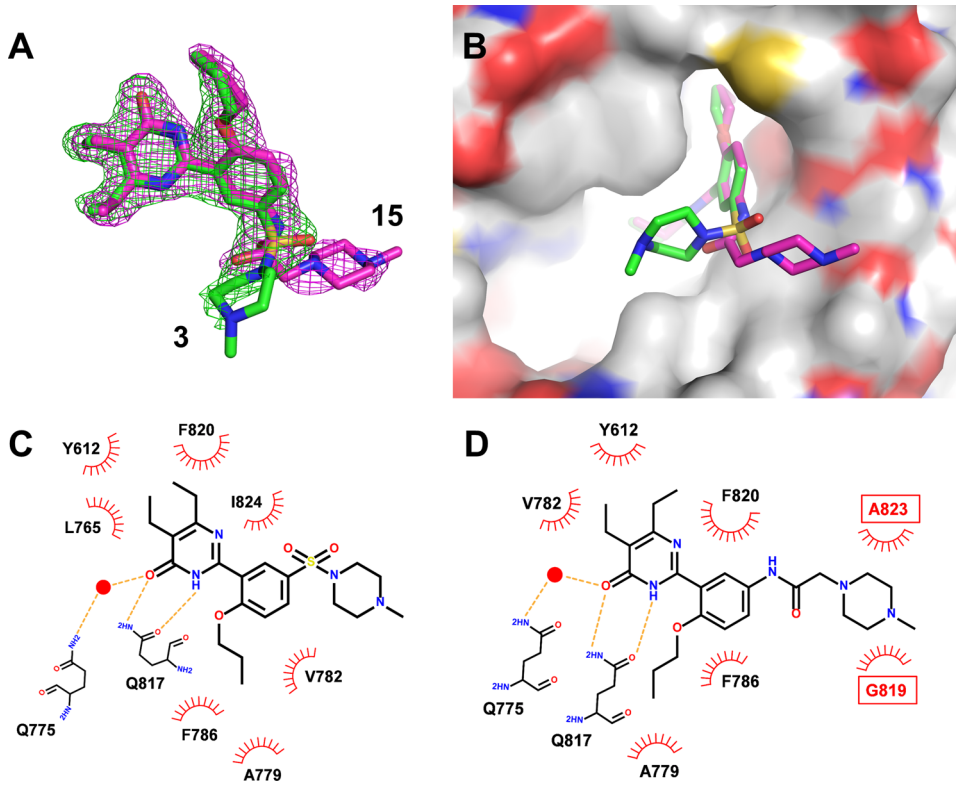

Figure 1. Crystal structures of the catalytic domain of PDE5 in complex with compounds **3** (green, PDB code: 4G2W) and **15** (magenta, PDB code: 6IWI). (A) $F_o - F_c$ difference electron-density maps contoured at 3.0σ for two compounds bound in PDE5. (B) Molecular surface of the ligand binding pockets of PDE5 with two compounds. (C, D) LIGPLOT representation of detailed interactions formed between the protein and compounds (C) **3** or (D) **15**.[31]

adenosine monophosphate (cAMP) and cGMP.[24] High selectivity is thus crucial to a PDE5 inhibitor as each PDE isozyme acts as a key element in regulation of some physiological processes, and inhibition of other PDE isozymes rather than PDE5 may lead to off-target-based adverse effects.[25] Both sildenafil and tadalafil serve as effective therapeutics for PAH as monotherapy or a key component of combination therapy; however, their clinical usefulness has been limited due to the excessive side effects mostly derived from the unsatisfactory selectivity across multiple PDEs.[26−29] In addition, the approved dose of sildenafil for the treatment of PAH is 20 mg t.i.d. because of its short half-life.[30] Considering that PAH is a chronic disease, it is of paramount importance to acquire a convenient and safe oral once-daily therapy. Accordingly, on the basis of a lead compound (**3**) from our previously reported 4(3*H*)-pyrimidinones, we continued our project aiming to find a novel PDE5 inhibitor with more potential therapeutic benefits in PAH treatment by improving the pharmacokinetics properties as well as selectivity of the compound.[21]

RESULTS AND DISCUSSION

Design of Aminosulfonylphenyl Pyrimidones. Among our previously reported inhibitors, compound **3** (5,6-diethyl-2-[2-*n*-propoxy-5-(4-methyl-1-piperazinylsulfonyl)phenyl]-pyrimid-4(3*H*)-one) stands out as a highly potent and selective PDE5 inhibitor (IC_{50} = 1.6 nM) and exhibits a good efficacy in the animal model. However, the pharmacokinetics study revealed that the compound had an insufficiently long terminal half-life ($t_{1/2}$ = 1.29 h) and a poor oral bioavailability (F = 10%) in rats, preventing it from being a candidate for clinical studies.[21] Our major efforts are thereby devoted to improving the pharmacokinetics properties of this congeneric series. Earlier SAR studies have already demonstrated that the 5,6-diethyl-pyrimidin-4(3*H*)-one of **3** exhibits the strongest inhibition potency among the pyrimidin-4(3*H*)-one analogues and the *n*-propoxyl substituent at the 2′-position of the phenyl ring contributes to the favorable hydrophobic interactions with the enzyme. Moreover, the determined crystal structure of the catalytic domain of PDE5 in complex with **3** (PDB code: 4G2W) indicates that it fits well into the ligand binding pocket except for the methylpiperazine group, which extended out into a solvent-exposed surface region and had rare interactions with the protein surroundings (Figure 1A−C). It is in line with a sparse electron-density associated with the methylpiperazine ring. From these observations, we presumed that further modifications for improvement of the pharmacokinetics properties should be performed on the methylpiperazine moiety to minimize the effect on potency and selectivity of the compound.

To test our conjecture, we first replaced the methylpiperazine ring of compound **3** with three different substituents, resulting in compounds **4**−**6** (Scheme 1 and Table 1). Opening of the methylpiperazine ring and attachment of a basic morpholine to keep the three-bond linker between two nitrogen atoms resulted in compound **4**. In addition, an acidic carboxyl was introduced on the α and β positions of the N atom of sulfonamide to make compounds **5** and **6**, respectively. An in vitro enzyme activity assay showed that three compounds all retained the potency (IC_{50} of 1.01, 2.02, and 1.69 nM for **4**, **5**, and **6**, respectively) as high as that of **3**, while their inhibition selectivity over PDE6 varied (Table 1). Among

DOI: 10.1021/acs.jmedchem.9b00123
J. Med. Chem. 2019, 62, 4979−4990

Scheme 1. Synthesis of Compounds 4−6[a]

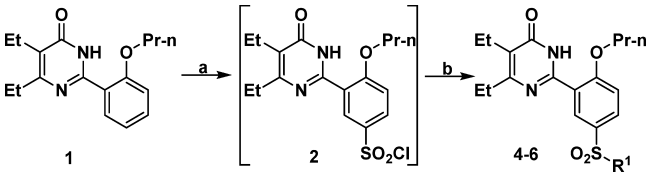

[a]Reagents and conditions: (a) chlorosulfonic acid, 5 °C; (b) amines, Et_3N, dichloromethane.

Table 1. Chemical Structure, PDE5/PDE6 Inhibitory Activity, and Metabolic Stability in Human Liver Microsome (HLM%) of Aminosulfonylphenyl Pyrimdinones (3−6)

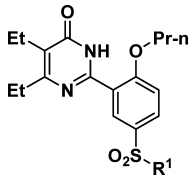

Compds	R^1	$IC_{50(PDE5)}$ (nM)	$IC_{50(PDE6)}/IC_{50(PDE5)}$	HLM (%)
3	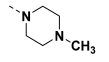	1.60	39	29%
4	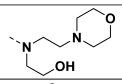	1.01	10	/
5		2.02	20	/
6	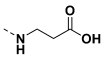	1.69	86	100%

them, compound **6** exhibits an outstanding selectivity over PDE6 (86-fold), which is more than double that of **3** (39-fold). The in vitro human liver microsome (HLM) metabolic stability test has been extensively used in drug discovery projects to evaluate the metabolic stability of a compound in development. Such a test was thus performed on compound **6**. To our surprise, no metabolism of **6** was found after 30 min of incubation in the HLM (HLM% = 100%), while only 29% of **3** remained at the same condition (Table 1), suggesting that compound **6** is extremely stable in HLM. Higher stability and better selectivity of **6** over compound **3** prompt us to carry out an investigation on the in vivo efficacy of compound **6** in a male spontaneously hypertensive rat (SHR) model. Unfortunately, it does not show an expected efficacy in vivo (Figure 2A) possibly due to the strong polarity of the carboxylic group resulting in poor membrane permeability and oral absorption.

Design of Aminophenylpyrimidones. Substitution of the methylpiperazine ring confirmed that this moiety can be replaced by other groups without sacrificing the potency. In addition, according to the crystal structure of PDE5 in complex with **3**, the sulfone group has no interaction with the protein, and its orientation prevents the methylpiperazine ring from making contact with the protein surface, leading us to think about a further replacement of the sulfone group. Considering a smaller size for less steric obstruction and synthetic ease for further modification, an amine group was introduced to replace the sulfone (Scheme 2 and Table 2). Compound **9**, with an unsubstituted amino group on the benzene ring, had single-digit nanomolar potency against PDE5 (IC_{50} = 5.33 nM) and demonstrated a moderate selectivity over PDE6 (10-fold). As the amino group on a benzene ring often leads to adverse effect on the pharmacokinetics property and safety of the compound, a carbonyl connected with different substituents was subsequently designed to yield amides **10**−**13**, **15**, and **16**. Except for compound **10**, a second nitrogen with a form of a tertiary amine or an amide was introduced and the length of the linker between two nitrogen atoms varied in the other five compounds. Again, these compounds retain the high potency against PDE5; in particular, most compounds exhibiting a subnanomolar potency (IC_{50} values of 0.54, 0.79, 0.92, and 0.62 nM for **11**, **12**, **13**, and **15**, respectively). The selectivity of these compounds against PDE5 over PDE6 showed greater variability, ranging from 7- to 32-fold, and compound **15** demonstrated the best one with a 32-fold selectivity over PDE6. The in vitro HLM metabolic stability test showed that **15** with an HLM% of 91% was much more stable than compound **3** after 30 min of incubation in the HLM. Therefore, compound **15** was selected for further investigation.

In addition, substitution at the NH_2 group of **9** using other functional groups to form urea (**17** and **18**), oxalic amide (**19** and **20**), and sulfamide (**21**) was carried out (Table 2). As expected, these compounds have nanomolar or subnanomolar inhibitory activities against PDE5 and moderate selectivity over PDE6. Among them, compound **21** shows a 28-fold selectivity

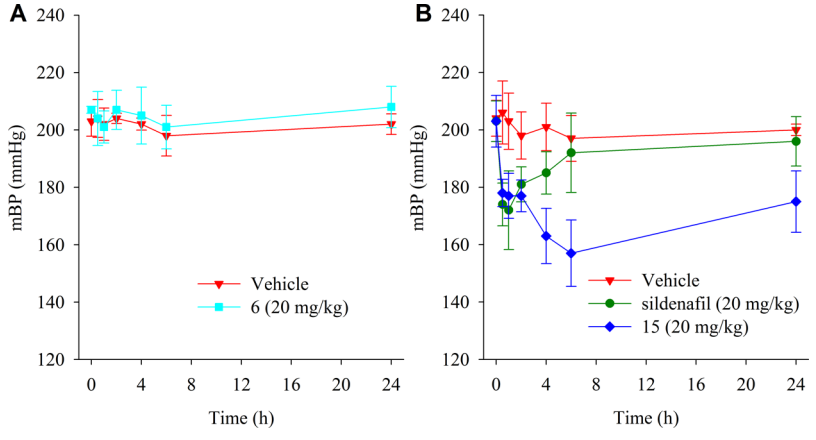

Figure 2. Effect of compound (A) **6** and (B) **15** on mean arterial blood pressure in an SHR model (mean ± SD, n = 6). Sildenafil was used as a reference. Normal saline was taken as a vehicle.

DOI: 10.1021/acs.jmedchem.9b00123
J. Med. Chem. 2019, 62, 4979−4990

Scheme 2. Synthesis of Compounds 7−21[a]

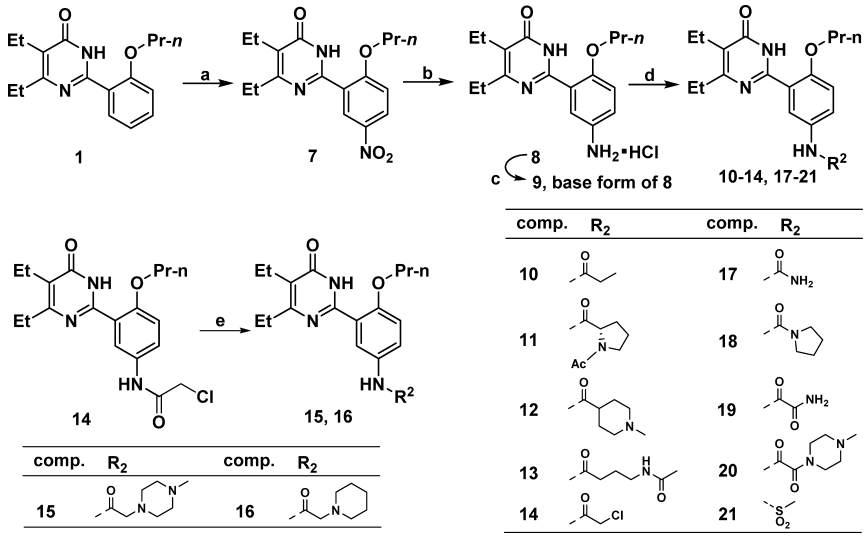

[a]Reagents and conditions: (a) conc. H_2SO_4, conc. HNO_3, 5 °C, 90%; (b) H_2, 10% Pd/C, HCl gas, methanol, r.t., 97%; (c) 0.4 N NaOH, 86%; (d) for **10**−**13**, acids, Et_3N, EDCI, HOBT, dichloromethane, r.t.; for **14**, **18**, and **21**, acyl chloride or methylsulfonyl chloride, Et_3N, dichloromethane, 0 °C; for **17**, KCNO, HOAc, reflux, 91%; for **19** and **20**, ethyl oxalyl monochloride, Et_3N, dichloromethane, 0 °C, then amines, methanol; (e) amines, Et_3N, DMF, 60 °C.

Table 2. Chemical Structure, PDE5/PDE6 Inhibitory Activity, and HLM% of Aminophenylpyrimdinones (9−21)

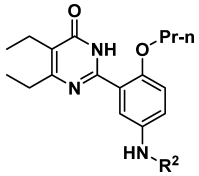

Compds	R^2	$IC_{50(PDE5)}$ (nM)	$IC_{50(PDE6)}/IC_{50(PDE5)}$	HLM (%)
9	−−H	5.33	10	/
10		1.21	11	/
11		0.54	10	/
12		0.79	24	/
13	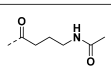	0.92	7	/
15	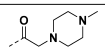	0.62	32	91%
16		1.46	9	/
17		1.61	17	/
18		1.86	11	/
19		0.83	22	/
20	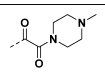	1.55	17	/
21		1.23	28	27%

over PDE6 but is unfortunately not so stable in the HLM (HLM% = 27%).

Structural and Thermodynamic Characterization of 15 Binding to PDE5. As mentioned above, the introduction of the amino group instead of the sulfone aims to reduce the steric obstruction and to establish more interactions of the substituent with the protein surface. To test the idea, we determined the crystal structure together with the thermodynamic profiles of the catalytic domain of PDE5 binding to compounds **3** and **15** (Tables 3 and 4 and Figure 1, PDB code: 6IWI). As expected, the carbonyl oxygen of **15** adopted an orientation opposite to that of the sulfone oxygen of **3** so that the following *N*,*N*-dimethylpiperazine moiety could lay down the protein surface and form hydrophobic interactions with residues G819 and A823 (Figure 1). This provides an explanation for the higher in vitro potency of **15** over **3** as the terminal methylpiperazine ring of **3** has no interaction with the protein (Figure 1). Consistent with the structure information, the binding enthalpy of **15** with PDE5 measured by isothermal titration calorimetry (ITC) experiments is more significant compared to **3**, whereas the interactions established between the *N*,*N*-dimethylpiperazine group and the surrounding residues lead to more entropic losses associated with **15** than with **3** (Table 4). Consequently, the total binding free energy of **15** with PDE5 is slightly stronger compared to **3**. Altogether, the structural and thermodynamic data of two compounds are not only in line with their IC_{50} but also help to gain deep insight into the essential factor responsible for the different potencies, rationalizing our strategy for use of the amino group instead of the sulfone.

Inhibitory Selectivity of 15 over 11 PDEs. We measured the selectivity profile of compound **15** against 11 human recombinant PDEs (Table 5) by comparing its in vitro potency for PDE5 to its inhibition of other PDEs. Sildenafil and tadalafil were used as reference inhibitors, and their selectivity indexes across 11 PDEs were also evaluated in parallel. The IC_{50} values of **15**, sildenafil, and tadalafil toward PDE5 are 0.62, 4.31, and 2.35 nM, respectively. Compound **15** showed an excellent selectivity over PDE2, **3**, **4**, **7**, **8**, **9**, and **10** (>16,129-fold). Remarkably, a 1610-fold selectivity of **15**

DOI: 10.1021/acs.jmedchem.9b00123
J. Med. Chem. 2019, 62, 4979−4990

Table 3. Crystallography Data Collection and Refinement Statistics

data Collection	PDE5/15
PDB ID	6IWI
space group	$P3_12_1$
cell constants	
a (Å)	74.75
b (Å)	74.75
c (Å)	132.02
wavelength (Å)	0.979
resolution range (Å)	36.39−2.15 (2.25−2.15)[a]
redundancy	18.9 (17.5)
I/σ (I)[b]	6.9 (3.2)
completeness (%)	94.23 (57.88)
refinement	
R_{work}/R_{free}[c]	0.185/0.227
reflections (unique)	22358
RMS values	
bond length (Å)	0.002
bond angle (°)	0.435
protein atoms	2313
ligands	2
water molecules	146
clashscore	1.32
MolProbity score	0.86
Ramachandran plot	
favored (%)	99.65
allowed (%)	0.35
outliers (%)	0.00

[a]Statistics for the highest-resolution bin of reflections in parentheses. [b]Intensity, signal-to-noise ratio. [c]R_{free} is calculated against a 5% random sampling of the reflections that were removed before structure refinement.

toward PDE11 was found, which is much more selective than tadalafil (9-fold). In addition, the selectivity of **15** over PDE1 as well as PDE6 was higher than sildenafil (5871-fold vs 190-fold to PDE1 and 32-fold vs 8-fold to PDE6). Overall, the potency and the selectivity of **15** over 11 PDEs are superior to those of sildenafil and tadalafil, implying that fewer side effects from the treatment with **15** can be anticipated.

Pharmacokinetic Profiles of 15. Pharmacokinetic profiles of compound **15** in rats and dogs were comprehensively evaluated and summarized in Table 6. After oral administration of a 1 mg/kg dose of **15** to Sprague−Dawley rats (three males and three females), a T_{max} of 2.8 h, a C_{max} of 43.9 ng/mL, an AUC_{0-t} of 268 ng/h/mL, an $AUC_{0-\infty}$ of 284 ng/h/mL, an MRT of 5.56 h, a $t_{1/2}$ of 2.82 h, and an oral bioavailability of 66.4% were obtained. The same experiment with intravenous administration of **15** suggested that it has a moderate plasma clearance (CL = 2.26 L/h/kg) and high volume of distribution (Vss = 4.97 L/kg). Moreover, the pharmacokinetic profile of **15** with a dose of 0.5 mg/kg in beagle dogs is more desirable than in rats. After intravenous administration to dogs (three males and three females), a much lower plasma clearance (CL = 0.648 L/h/kg) and a similar volume of distribution (Vss = 3.83 L/kg) were observed compared with the higher dose administration to rats, leading to a longer terminal half-life ($t_{1/2}$ = 4.89 h) in dogs than in rats. Additionally, **15** maintained the good oral bioavailability of 67% after oral administration to dogs. The promising pharmacokinetic properties of **15** in rats as well as in dogs warrant further evaluation of its therapeutic potential in PAH as well as other PDE5-associated diseases.

Some pharmacokinetics data of sildenafil and tadalafil reported previously were also listed in Table 6 for comparison. The terminal half-life of **15** in rats is longer than that of sildenafil and is comparable to tadalafil. The oral bioavailability of **15** in rats is much better than that of sildenafil and is similar to that of tadalafil. In addition, in healthy volunteers, the terminal half-lives of sildenafil and tadalafil after oral administration are 3.7 and 17.5 h, respectively. Taking the preclinical and clinical pharmacokinetics data of sildenafil and tadalafil together with the preclinical pharmacokinetic profile of **15**, we speculated that the human terminal half-life of **15** would be more than 10 h. As anticipated, in our phase I first-in-man clinical trials (registration no. CTR20171238, http://www.chinadrugtrials.org.cn), it did show a terminal half-life of 10.9 h after oral administration of 5 mg of **15**. Accordingly, the excellent pharmacokinetics data of compound **15** lay a good foundation for a once-daily oral dosing profile of **15** for the treatment of PAH.

In Vivo Efficacy of 15 in Animal Models. The in vivo efficacy of compound **15** was first investigated in an acute model of hypertension in spontaneously hypertensive rats (SHRs).[14] Figure 2B shows that in the first 2 h, **15** and sildenafil exerted an equivalent effect of a drop in blood pressure of SHRs; such a drop effect was further reinforced for **15** but was attenuated for sildenafil in the next couple of hours, and the apparent antihypertensive effect of **15** was maintained over 24 h, while sildenafil hardly had any efficacy after 6 h. Hence, treatment with **15** rapidly and remarkably decreases the blood pressure of SHR, and such an antihypertensive effect is maintained for a long time, gaining a much more robust efficacy than sildenafil in SHRs.

Subsequently, effects of compound **15** against PAH were evaluated in a monocrotaline (MCT)-induced PAH rat model.[32] Sildenafil and bosentan, targeting the nitric oxide and endothelin pathways, respectively, are the first-line oral drugs for the treatment of PAH. They were used in our studies as the positive control. After 21 consecutive days of injection of MCT, a significant increase of the mean pulmonary artery pressure (mPAP) was observed in the model group compared with that in the control group ($p < 0.01$), demonstrating that the application of MCT successfully induced the symptom of PAH. Treatment with compound **15**, sildenafil, and bosentan all apparently decreased the mPAP of the rats (Figure 3). Administration of **15** showed the efficacy comparable to that of sildenafil or bosentan; however, its dose (1 mg/kg) was much lower than that of sildenafil (25 mg/kg) or bosentan (100 mg/kg), which is principally due to its high in vitro PDE5 activity. Taken together, these data demonstrated the robust efficacy of

Table 4. Thermodynamic Properties of Compounds 3 and 15 Binding to PDE5

compds	K_d (M)	ΔG (kJ/mol)	ΔH (kJ/mol)	$-T\Delta S$ (kJ/mol)	IC_{50} (nM)
3	$1.31 \pm 0.05 \times 10^{-7}$	−39.86 ± 0.09	−70.35 ± 3.43	30.49 ± 3.45	1.6
15	$0.82 \pm 0.03 \times 10^{-7}$	−41.06 ± 0.26	−90.07 ± 1.35	49.01 ± 1.16	0.62

DOI: 10.1021/acs.jmedchem.9b00123
J. Med. Chem. 2019, 62, 4979−4990

Table 5. In Vitro Activities and Selectivities of 15, Sildenafil, and Tadalafil to 11 PDE Enzymes (Mean ± SD, n = 3)

	15		sildenafil		tadalafil	
PDEs	IC_{50} (nM)	selectivity[a]	IC_{50} (nM)	selectivity[a]	IC_{50} (nM)	selectivity[a]
PDE1	3640 ± 215	5871	819 ± 89	190	>10000	>4255
PDE2	>10000	>16129	>10000	>2320	>10000	>4255
PDE3	>10000	>16129	>10000	>2320	>10000	>4255
PDE4	>10000	>16129	>10000	>2320	>10000	>4255
PDE5	0.62 ± 0.13		4.31 ± 0.46		2.35 ± 0.28	
PDE6	19.8 ± 7.7	32	36.4.2 ± 1.8	8	402 ± 56	171
PDE7	>10000	>16129	>10000	>2320	>10000	>4255
PDE8	>10000	>16129	>10000	>2320	>10000	>4255
PDE9	>10000	>16129	>10000	>2320	>10000	>4255
PDE10	>10000	>16129	>10000	>2320	>10000	>4255
PDE11	998 ± 192	1610	4930 ± 1140	1144	22.1 ± 5.9	9

[a]Selectivity, $IC_{50(PDEs)}/IC_{50(PDE5)}$.

compound **15** in two animal models and thus promoted a further development of this compound into clinically therapeutic applications.

Chemistry. The synthesis of compounds **4**, **5** and **6** was pursued with a similar protocol as previously reported (Scheme 1).[21] The key intermediate **2** was freshly prepared by the treatment of **1** with chlorosulfonic acid at 0 °C.[33] The sulfonylation reactions of amines by **2** were accomplished with triethylamine as a base in dichloromethane. The selective nitration at the C5 position of benzene ring of compound **1** in the mixture of concentrated sulfuric acid and concentrated nitric acid at 5 °C gave **7** with satisfying yield and purity. The reduction of **7** in methanol under a hydrogen atmosphere gave crude **9**. The solution of crude **9** in methanol was treated with dried hydrogen chloride gas to form **8** (salt form of 9), and the purification of **8** was achieved by the crystallization in methanol. Purified **8** was alkalized in water to furnish **9** with high purity (Scheme 2). Because **8** has better stability than **9** at the same storage condition, it was used as the key intermediate for synthesis of compounds **10**–**21**. Compounds **10**–**13** were prepared by condensation of **8** with propanoic acid, *N*-acetyl-L-proline, 1- methyl-4-piperidinecarboxylic acid, or 4-(acetylamino)butanoic acid, respectively, in the presence of 1-(3-dimethylaminopropyl)-3-ethylcarbodiimide and 1-hydroxybenzotriazole. Compound **8** is acylated with chloroacetyl chloride to give **14**, which is the intermediate to produce compounds **15** and **16** by alkylation of the *N*-methylpiperazine and piperidine, respectively. Compound **17** was obtained by a reaction of **8** with potassium cyanate in the presence of acetic acid. Compound **8** was treated with pyrrolidine-1-carbonyl chloride and dichloromethane using triethylamine as the base to furnish **18**. **19** and **20** were furnished by acylation of **8** by ethyl oxalyl monochloride, followed by ammonolysis reaction with ammonia or *N*-methylpiperazine, respectively. Sulfonylation of **8** by methanesulfonyl chloride in dichloromethane gave **21** (Scheme 2).

CONCLUSIONS

Given the effectiveness of PDE5 as a key target for PAH, ED, and new indications discovered, both in academia and the pharmaceutical industry, there is continuous interest in the discovery of novel PDE5 inhibitors with fewer side effects. Here, we present the development of compound **3**, a potent and selective PDE5 inhibitor reported previously, into a clinical candidate (compound **15**, also named TPN171) with major effort devoted to optimizing the pharmacokinetic profile of the compound. As design of new compounds with desirable pharmacokinetic properties has proved to be challenging and the crystal structure suggests that the methylpiperazine-substituted sulfone of **3** hardly interacts with the enzyme, small modifications on this moiety were performed. Two major congeneric series of **3**, 3 aminosulfonylphenylpyrimidones and 13 acylaminophenylpyrimidones were designed, synthesized, and assessed in terms of their PDE5 and PDE6 activities. All compounds retained the high potency against PDE5 as their IC_{50} values range from single-digit nanomolar to subnanomolar. Only compounds with selectivity over PDE6 comparable to or better than **3** were filtered by an in vitro HLM metabolic stability test, and the metabolically stable compounds were further investigated in animals to evaluate the in vivo pharmacokinetics and efficacies for PAH. Through these efforts, we were able to identify TPN171 (compound **15**), which possesses multiple drug-like properties such as high potency, outstanding selectivity, well-characterized mechanism of action, excellent pharmacokinetic profile, and easy preparation of the active pharmaceutical ingredient (API), warranting further evaluation of its therapeutic potential in clinical trials. A phase II clinical trial is now underway to test its safety and efficacy in PAH patients.

EXPERIMENTAL SECTION

All commercially available materials and solvents were used without any further purification. TLC analyses were performed on Merck silica gel 60 F254 plates. ^{1}H NMR spectra and ^{13}C NMR spectra were recorded at room temperature on a Bruker AMX-400 using TMS as an internal standard. Mass spectra were recorded on a Finnigan MAT-95/711 spectrometer. The purity of test compounds were determined by HPLC (Agilent ChemStation, Aigent ZORBAX RX-C8 4.6 × 250 mm, 5 μm, 30 °C, flow rate = 1.0 mL/min) with aqueous CH3CN (25–72%, 0.1% FA) for 30 min. The purity of all synthesized compounds is not less than 95%.

General Procedure for the Synthesis of 4–6. Compound **1** (1 mmol) was slowly added into chlorosulfonic acid (5 mL) at 5 °C, after stirring at room temperature for 2 h, and the reaction mixture was added dropwise into brash ice to generate a faint yellow precipitate. The solid was collected by filtration, washed with ice water, and dried under reduced pressure to give crude **2**. The crude **2** was dissolved in dichloromethane (50 mL) and added dropwise into dichloromethane (30 mL) containing amine (1.1 mmol) and triethylamine (1 mL) at 5 °C, followed by stirring for 30 min; the organic phase was washed with water (3 × 20 mL) and saturated brine (20 mL), and the solvent was evaporated off to dryness to give the residue. Melting points were taken in an open capillary on RY-1G apparatus and were uncorrected.

DOI: 10.1021/acs.jmedchem.9b00123
J. Med. Chem. 2019, 62, 4979–4990

Table 6. Pharmacokinetic Profiles of 15, Sildenafil, and Tadalafil

compounds	species	Route	dose (mg/kg)	T_{max} (h)	C_{max} (ng/mL)	AUC_{0-t} (ng/h/mL)	$AUC_{0-\infty}$ (ng/h/mL)	MRT (h)	$t_{1/2}$ (h)	CL (L/h/kg)	Vss (L/kg)	F (%)
15[a]	rats	IV	1.0			403 ± 47	412 ± 51	2.22 ± 0.23	2.4 ± 0.37	2.26 ± 0.28	4.97 ± 0.18	
		PO	1.0	2.8 ± 0.4	43.9 ± 11.6	268 ± 83	284 ± 82	5.56 ± 0.51	2.82 ± 0.61			66.4
	dogs	IV	0.5			752 ± 272	773 ± 289	6.07 ± 0.84	4.5 ± 0.51	0.648 ± 0.175	3.83 ± 0.77	
		PO	0.5	1.9 ± 0.7	66.5 ± 14.1	495 ± 148	514 ± 164	7.21 ± 1.05	4.89 ± 1.09			67.0
sildenafil[b]	rats	IV	4.0						1.1	1.83	1.6	
		PO	1.0	1.6	76				0.65			34
tadalafil[c]	rats	IV							2.4	0.31	5.2	
		PO										63

[a]Pharmacokinetic profiles of **15** were determined as described in the Experimental Section; data are expressed as mean ± SD, $n = 6$. [b]Pharmacokinetic profiles of sildenafil are taken from the literature, and data are the arithmetic average of the males and females.[30] [c]Pharmacokinetic profiles of tadalafil are taken from the literature.[13]

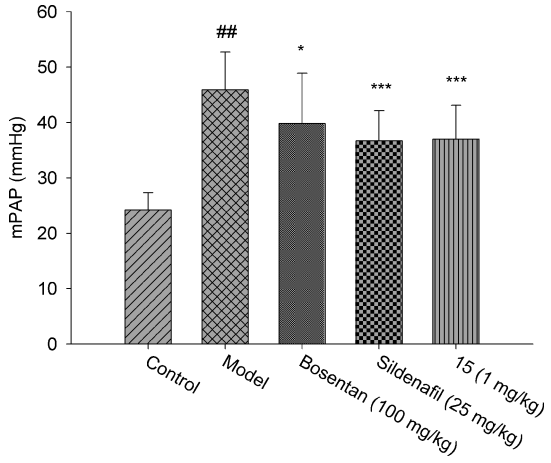

Figure 3. Effects of **15** on mean pulmonary arterial pressure (mPAP) in a MCT rat model. Bosentan and sildenafil were used as references. The data are expressed as the mean ± SD ($n = 20$/group). ##: $P < 0.01$ compared with the control group; *: $P < 0.05$, ***: $P < 0.001$ compared with the model group.

5,6-Diethyl-2-(2-*n*-propoxy-5-(*N*-(2-morpholinylethyl)-*N*-(2-hydroxyethyl) aminosulfonyl)phenyl)-4(3*H*)-pyrimidone (4). The amine was 2-(2-morpholinoethylamino)ethanol, and the residue was recrystallized from ethyl acetate/hexane to give the title compound to give an off-white solid (291 mg, yield 56% over two steps). mp 76−77 °C. ^{1}H NMR ($CDCl_3$, 500 MHz): δ 10.97 (1H, br), 8.88 (1H, s), 7.90 (1H, d, J = 8.5 Hz), 7.15 (1H, d, J = 9.0 Hz), 6.25 (1H, br), 4.25 (2H, t, J = 6.0 Hz), 3.83 (2H, s), 3.76 (4H, s), 3.28 (2H, s), 3.22 (2H, s), 2.59−2.74 (10H, m), 2.03 (2H, m), 1.28 (3H, t, J = 7.0 Hz), 1.16 (6H, m); ^{13}C NMR ($CDCl_3$, 125 MHz): δ 164.45, 162.08, 160.13, 149.82, 131.87, 131.11, 130.59, 125.20, 120.55, 113.15, 71.91, 66.38, 62.85, 57.81, 53.41, 53.38, 47.30, 27.52, 22.26, 18.73, 13.31, 13.05, 10.57; LRMS m/z 523.4 $[M + H]^+$; HRMS (ESI) m/z calculated for $C_{25}H_{39}N_4O_6S$ $[M + H]^+$ 523.2585, found 523.2594; HPLC purity 97.76%, t_r = 21.99 min.

***N*-(3-(5,6-Diethyl-4(3*H*)-pyrimidone-2-yl)-4-*n*-propxyphenylsulfonyl-L-proline (5).** The amine was L-proline, and the crude product was recrystallized from ethyl acetate/hexane to give the title compound to give an off-white solid (282 mg, yield 61% over two steps). mp 172−174 °C. ^{1}H NMR (CD_3OD, 500 MHz): δ 8.32 (1H, d, J = 2.0 Hz), 8.05 (1H, dd, J = 8.5, 2.0 Hz), 7.36 (1H, d, J = 9.0 Hz), 4.22 (2H, t, J = 6.5 Hz), 4.09 (1H, m), 3.55 (1H, m), 3.34 (1H, m), 2.73 (2H, q, J = 7.5 Hz), 2.62 (2H, q, J = 7.5 Hz), 1.91 (5H, m), 1.65 (1H, m), 1.31 (3H, t, J = 7.5 Hz), 1.17 (3H, t, J = 7.5 Hz), 1.08 (3H, t, J = 7.0 Hz); ^{13}C NMR (CD_3OD, 125 MHz): δ 164.24, 164.17, 164.08, 160.21, 152.32, 132.09, 130.16, 129.94, 124.02, 121.57, 113.04, 71.03, 63.25, 48.87, 31.24, 26.69, 24.39, 22.01, 21.95, 18.11, 12.35, 9.49; LRMS m/z 464.3 $[M + H]^+$; HRMS (ESI) m/z calculated for $C_{22}H_{30}N_3O_6S$ $[M + H]^+$ 464.1850, found 464.1863; HPLC purity 96.38%, t_r = 16.98 min.

2-(*N*-(3-(5,6-Diethyl-4(3*H*)-pyrimidone-2-yl)-4-*n*-propoxyphenyl)sulfonyl)aminopropanoic Acid (6). The amine was 3-aminopropanoic acid, and the crude product was recrystallized from ethyl acetate/hexane to give the title compound as an off-white solid (262 mg, yield 60% over two steps). mp 186−187 °C. ^{1}H NMR (CD_3OD, 500 MHz): δ 8.24 (1H, d, J = 2.5 Hz), 7.88 (1H, dd, J = 8.5, 2.0 Hz), 7.24 (1H, d, J = 9.0 Hz), 4.12 (2H, t, J = 6.5 Hz), 3.02 (2H, t, J = 7.0 Hz), 2.61 (2H, q, J = 7.5 Hz), 2.50 (2H, q, J = 7.5 Hz), 2.37 (2H, t, J = 7.0 Hz), 1.80 (2H, m), 1.19 (3H, t, J = 7.5 Hz), 1.05 (3H, t, J = 7.5 Hz), 0.96 (3H, t, J = 6.0 Hz); ^{13}C NMR (CD_3OD, 125 MHz): δ 173.54, 164.37, 163.69, 159.99, 152.12, 132.58, 131.51, 129.56, 124.04, 121.53, 112.95, 71.06, 38.56, 34.05, 26.79, 21.94, 18.10, 12.31, 12.27, 9.45; LRMS m/z 438.3 $[M + H]^+$; HRMS (ESI) m/z calculated for $C_{20}H_{28}N_3O_6S$ $[M + H]^+$ 438.1693, found 438.1704; HPLC purity 96.29%, t_r = 15.19 min.

DOI: 10.1021/acs.jmedchem.9b00123
J. Med. Chem. 2019, 62, 4979−4990

2-(5-Nitro-2-*n*-propoxyphenyl)-5,6-diethyl-4(3*H*)-pyrimidone (7). The compound **1** (40 mmol) was dissolved in concentrated sulfuric acid (100 mL) under an ice bath, and concentrated nitric acid (100 mL) was slowly added. After stirring at room temperature for 3 h, the reaction mixture was slowly added dropwise into ice water to generate a light yellow precipitate. After filtration, the solid was washed with water (3 × 200 mL) and dried at 60 °C to give the title compound **7** as a yellow solid (11.92 g, yield: 90%). mp 138−139 °C. ^{1}H NMR ($CDCl_3$, 500 MHz): δ 11.32 (1H, br), 9.20 (1H, d, J = 3.0 Hz), 8.34 (1H, dd, J = 9.0, 3.0 Hz), 7.16 (1H, d, J = 9.0 Hz), 4.28 (1H, t, J = 6.5 Hz), 2.71 (2H, q, J = 7.5 Hz), 2.58 (2H, q, J = 7.5 Hz), 2.02 (2H, m), 1.31 (3H, t, J = 7.5 Hz), 1.14 (6H, m); ^{13}C NMR ($CDCl_3$, 125 MHz): δ 164.68, 162.37, 161.43, 149.74, 141.84, 127.85, 127.26, 125.18, 120.85, 112.86, 72.16, 27.61, 22.22, 18.71, 13.27, 13.14, 10.48; LRMS m/z 332.3 $[M + H]^+$.

2-(5-Amino-2-*n*-propoxyphenyl)-5,6-diethyl-4(3*H*)-pyrimidone Hydrochloride (8) and 2-(5-Amino-2-*n*-propoxyphenyl)-5,6-diethyl-4(3*H*)-pyrimidone (9). The compound 7 (16.5 g, 50 mmol) was dissolved in methanol, 0.4 g of 10% Pd/C was added, and the solution was hydrogenized at ambient temperature and pressure. When hydrogen was not absorbed by the reaction mixture anymore, Pd/C was filtered off. The filtrate was concentrated to a small volume and fed with dried HCl gas to generate a white solid, which was collected by filtration and dried to give the title compound **8** (16.4 g, yield: 97%). The compound **8** (337 mg, 1 mmol) was stirred in 0.4 N NaOH solution (5 mL, 2 mmol), the precipitate was collected by filtration, and the cake was washed with 2 mL of water to give **9** as a white solid (257 mg, yield: 86%). mp 79−80 °C. ^{1}H NMR ($CDCl_3$, 400 MHz): δ 11.27 (1H, br), 7.85 (1H, d, J = 2.8 Hz), 6.85 (2H, m), 4.08 (2H, d, J = 6.4 Hz), 3.62 (2H, br), 2.68 (2H, q, J = 7.2 Hz), 2.59 (2H, q, J = 7.2 Hz), 1.96 (2H, m), 1.31 (3H, t, J = 6.0 Hz), 1.15 (6H, m); ^{13}C NMR (CD_3OD, 125 MHz): δ 165.64, 163.03, 153.04, 150.12, 141.48, 123.15, 120.24, 120.13, 116.62, 114.26, 71.11, 27.13, 22.24, 18.03, 12.38, 12.22, 9.60; LRMS m/z 302.3 $[M + H]^+$; HRMS (ESI) m/z calculated for $C_{17}H_{23}N_3O_2$ $[M + H]^+$ 302.1897, found 302.1888; HPLC purity 98.53%, t_r = 13.99 min.

***N*-(3-(5,6-Diethyl-4(3*H*)-pyrimidone-2-yl)-4-propoxyphenyl)propionamide (10).** Propanoic acid (58 mg, 0.78 mmol) was dissolved in dichloromethane (20 mL), 1-ethyl-3-(3-dimethylaminopropyl)carbodiimide hydrochloride (EDCI, 130 mg, 0.78 mmol) and triethylamine (158 mg, 1.56 mmol) were added, and the solution was stirred for 0.5 h. 1-Hydroxybenzotriazole (HOBT, 100 mg, 0.78 mmol) was added, and the solution was stirred for 12 h, followed by addition of **8** (262 mg, 0.78 mmol). After stirring at room temperature for 2 h, the reaction mixture was washed with water (10 mL) and saturated saline. The organic phase was dried with anhydrous Na_2SO_4 and concentrated under reduced pressure to give an oil, which was purified by fast chromatography (ethyl acetate/petroleum ether 1:10) to give the title compound as an off-white solid (250 mg, yield: 90%). mp 172−173 °C. ^{1}H NMR ($CDCl_3$, 500 MHz): δ 8.25 (1H, s), 8.01 (1H, dd, J = 9.0, 2.5 Hz), 7.81 (1H, s), 6.95 (1H, d, J = 9.0 Hz), 4.12 (1H, t, J = 7.0 Hz), 2.64 (2H, q, J = 8.0 Hz), 2.58 (2H, q, J = 8.0 Hz), 1.94 (2H, q, J = 7.0 Hz), 1.25 (6H, m), 1.13 (6H, m); ^{13}C NMR ($CDCl_3$, 125 MHz): δ 172.56, 164.34, 162.54, 153.69, 151.36, 132.43, 125.38, 124.09, 122.16, 119.23, 113.28, 71.35, 30.46, 27.58, 22.41, 18.71, 13.43, 13.15, 10.59, 9.75; LRMS m/z 380.3 $[M + Na]^+$; HRMS (ESI) m/z calculated for $C_{20}H_{28}N_3O_3$ $[M + H]^+$ 358.2125, found 358.2136; HPLC purity 97.02%, t_r = 16.46 min.

(2*S*)-1-Acetyl-*N*-(3-(5,6-diethyl-4(3*H*)-pyrimidone-2-yl)-4-*n*-propoxyphenyl)-2-pyrrolidine Carboxamide (11). The title compound was prepared in a similar manner to compound **10** using *N*-acetyl-L-proline instead of propanoic acid. Off-white solid (yield 66%). mp 141−143 °C. ^{1}H NMR ($CDCl_3$, 500 MHz): δ 9.63 (1H, s), 8.32 (1H, d, J = 2.0 Hz), 7.84 (1H, dd, J = 9.0, 2.0 Hz), 6.92 (1H, d, J = 9.0 Hz), 4.78 (1H, d, J = 7.5 Hz), 4.10 (2H, t, J = 6.5 Hz), 3.63 (1H, m), 3.49 (1H, m), 2.70 (2H, q, J = 7.5 Hz), 2.59 (3H, m), 2.17 (4H, m), 2.06 (1H, m),1.94 (3H, m), 1.30 (3H, t, J = 7.5 Hz), 1.15 (3H, t, J = 7.0 Hz), 1.11 (3H, t, J = 7.5 Hz); ^{13}C NMR ($CDCl_3$, 125 MHz): δ 171.61, 169.15, 164.35, 162.51, 153.58, 151.54, 132.44, 124.84, 124.11, 122.12, 119.39, 113.16, 71.31, 60.40, 48.55, 27.53, 27.12, 25.12, 22.58, 22.44, 18.71, 13.41, 13.31, 10.62; LRMS m/z 441.4 $[M + H]^+$; HRMS (ESI) m/z calculated for $C_{24}H_{33}N_4O_4$ $[M + H]^+$ 441.2496, found 441.2506; HPLC purity 98.51%, t_r = 14.37 min.

1-Methyl-*N*-(3-(5,6-diethyl-4(3*H*)-pyrimidone-2-yl)-4-*n*-propoxyphenyl)-4-piperidine Carboxamide (12). The title compound was prepared in a similar manner to compound **10** using 1-methyl-4-piperidinecarboxylic acid instead of propanoic acid. Off-white solid (210 mg, yield 63%). mp 94−95 °C. ^{1}H NMR (CD_3OD, 500 MHz): δ 8.17 (1H, d, J = 2.5 Hz), 7.84 (1H, dd, J = 9.0, 2.5 Hz), 7.26 (1H, d, J = 9.0 Hz), 4.15 (2H, 7, J = 6.5 Hz), 4.10 (2H, t, J = 6.5 Hz), 3.63 (2H, m), 3.15 (2H, m), 2.92 (3H, s), 2.81 (3H, m), 2.65 (2H, q, J = 7.5 Hz), 2.21 (2H, m), 2.08 (2H, m), 1.87 (2H, m), 1.35 (3H, t, J = 7.5 Hz), 1.20 (3H, t, J = 7.0 Hz), 1.05 (3H, t, J = 7.5 Hz); ^{13}C NMR (CD_3OD, 125 MHz): δ 172.58, 162.94, 155.17, 153.78, 131.86, 126.53, 124.59, 122.37, 122.29, 116.84, 113.29, 70.81, 53.40, 51.10, 42.66, 39.93, 26.31, 24.69, 24.16, 22.07, 18.05, 12.20, 11.96, 9.41; LRMS m/z 427.4 $[M + H]^+$; HRMS (ESI) m/z calculated for $C_{24}H_{35}N_4O_3$ $[M + H]^+$ 427.2704, found 427.2697; HPLC purity 98.62%, t_r = 15.15 min.

4-Acetylamino-*N*-(3-(5,6-diethyl-4(3*H*)-pyrimidone-2-yl)-4-*n*-propoxyphenyl) Butanamide (13). The title compound was prepared in a similar manner to compound **10** using 4-(acetylamino)-butanoic acid instead of propanoic acid. Off-white solid (228 mg, yield 68%). mp 142−143 °C.^{1}H NMR ($CDCl_3$, 500 MHz): δ 9.01 (1H, s), 8.48 (1H, d, J = 2.5 Hz), 7.90 (1H, dd, J = 9.0, 3.0 Hz), 6.95 (1H, d, J = 9.0 Hz), 6.32 (1H, s), 4.12 (2H, t, J = 6.5 Hz), 3.37 (2H, q, J = 4.8 Hz), 2.66 (2H, q, J = 7.5 Hz), 2.57 (2H, q, J = 7.5 Hz), 2.43 (2H, t, J = 6.5 Hz), 2.01 (3H, s), 1.94 (4H, m), 1.29 (3H, t, J = 7.5 Hz), 1.13 (6H, m); ^{13}C NMR ($CDCl_3$, 125 MHz): δ 171.68, 171.44, 163.98, 162.93, 153.66, 151.61, 132.63, 125.13, 123.96, 122.34, 119.30, 113.22, 71.36, 38.91, 34.70, 27.46, 26.16, 23.31, 22.44, 18.69, 13.41, 13.08, 10.63; LRMS m/z 429.4 $[M + H]^+$; HRMS (ESI) m/z calculated for $C_{23}H_{33}N_4O_4$ $[M + H]^+$ 429.2496, found 429.2506.

2-Chloro-*N*-3-(5,6-diethyl-4(3*H*)-pyrimidone-2-yl)-4-*n*-propoxyphenyl) Acetamide (14). The compound **8** (0.74 g, 2 mmol) was dissolved in dichloromethane (20 mL), triethylamine (2 mL) was added, followed by slow addition of chloroacetyl chloride (0.23 g, 2.05 mmol) at 0 °C. After stirring for 0.5 h, the reaction mixture was washed with water (10 mL), 1 N HCl (5 mL), saturated sodium bicarbonate solution (10 mL), and saturated saline. The organic phase was dried with anhydrous Na_2SO_4 and concentrated. The resultant oil was recrystallized from ethyl acetate−petroleum ether to give the compound **14** (0.71 g, yield: 94%). mp 161−162 °C. ^{1}H NMR ($CDCl_3$, 500 MHz): δ 8.41 (1H, br), 8.35 (1H, d, J = 3.0 Hz), 7.95 (1H, dd, J = 9.0, 3.0 Hz), 7.03 (1H, d, J = 9.0 Hz), 4.22 (2H, s), 4.16 (2H, t, J = 6.5 Hz), 2.69 (2H, q, J = 7.5 Hz), 2.58 (2H, q, J = 7.5 Hz), 1.97 (2H, m), 1.31 (3H, t, J = 7.5 Hz), 1.13 (6H, m); ^{13}C NMR ($CDCl_3$, 125 MHz): δ 164.09, 162.33, 154.558, 151.15, 151.14, 130.76, 125.56, 125.52, 124.52, 122.76, 119.49, 113.52, 71.49, 42.86, 27.53, 22.42, 18.74, 18.43, 13.39, 13.29, 10.63; LRMS m/z 378.3 $[M + H]^+$.

***N*-(3-(5,6-Diethyl-4(3*H*)-pyrimidone-2-yl)-4-*n*-propoxyphenyl)-2-(4-methylpiperazin-1-yl)acetamide (15).** The compound **14** (0.38 g, 1 mmol) was dissolved in a mixture of dimethylformide (3 mL) and triethylamine (202 mg, 2 mmol), and *N*-methylpiperazine (100 mg, 1 mmol) was added. The reaction mixture was heated to 60 °C for 10 h, concentrated to dryness, washed with water, and dried. The resultant solid was recrystallized from ethyl acetate−petroleum ether to obtain compound **15** as an off-white solid (278 mg, yield 63%). mp 134−136 °C.^{1}H NMR ($CDCl_3$, 500 MHz): δ 11.17 (1H, s), 9.12 (1H, s), 8.28 (1H, d, J = 2.0 Hz), 7.98 (1H, d, J = 9.0 Hz), 7.02 (1H, d, J = 9.0 Hz), 4.15 (2H, t, J = 7.0 Hz), 3.18 (2H, s), 2.71 (6H, m), 2.60 (6H, m), 2.38 (3H, s), 1.98 (2H, m), 1.32 (3H, t, J = 7.5 Hz), 1.14 (6H, m); ^{13}C NMR ($CDCl_3$, 125 MHz): δ 168.39, 164.34, 162.25, 153.92, 151.26, 131.64, 124.91, 124.41, 121.85, 119.66, 113.53, 71.43, 61.75, 55.07, 54.98, 53.21, 45.82, 27.65, 22.44, 18.73, 13.40, 13.14, 10.64; LRMS m/z 442.4 $[M + H]^+$; HRMS (ESI) m/z calculated for $C_{24}H_{36}N_5O_3$ $[M + H]^+$ 442.2813, found 442.2825; HPLC purity 98.80%, t_r = 11.98 min.

DOI: 10.1021/acs.jmedchem.9b00123
J. Med. Chem. 2019, 62, 4979−4990

***N*-(3-(5,6-Diethyl-4(3*H*)-pyrimidone-2-yl)-4-*n*-propoxyphenyl)-2-(piperidin-1-yl)acetamide (16).** The title compound was prepared in a similar manner to compound **15** using piperidine instead of *N*-methylpiperazine as an off-white solid (360 mg, yield: 82.5%). mp 140−141 °C. ^{1}H NMR ($CDCl_3$, 500 MHz): δ 11.17 (1H, s), 9.28 (1H, s), 8.29 (1H, d, J = 3.0 Hz), 7.99 (1H, dd, J = 9.0, 3.0 Hz), 7.02 (1H, d, J = 9.0 Hz), 4.16 (2H, t, J = 6.5 Hz), 3.10 (2H, s), 2.69 (2H, q, J = 7.5 Hz), 2.60 (6H, m), 1.98 (2H, m), 1.67 (2H, m), 1.50 (2H, m), 1.32 (3H, t, J = 7.5 Hz), 1.14 (6H, m); ^{13}C NMR ($CDCl_3$, 125 MHz): δ 169.07, 164.47, 162.27, 153.83, 151.29, 131.84, 124.83, 124.36, 121.78, 119.66, 113.51, 71.41, 62.74, 54.99, 27.67, 26.23, 23.65, 22.44, 18.72, 13.41, 13.17, 10.64; LRMS m/z 427.4 [M + H]$^+$; HRMS (ESI) m/z calculated for $C_{24}H_{35}N_4O_3$ [M + H]$^+$ 427.2704, found 427.2710; HPLC purity 98.50%, t_r = 19.02 min.

1-(3-(5,6-Diethyl-4(3*H*)-pyrimidone-2-yl)-4-*n*-propoxyphenyl)urea (17). The compound **8** (200 mg, 0.6 mmol) was suspended in a mixed solution of water (5 mL) and acetic acid (5 mL), potassium cyanate (81 mg, 1 mmol) was added, and the solution was heated to reflux and stirred for 2 h. The cooled reaction mixture was poured into water to generate a white solid, which was washed with water (10 mL × 3) and dried to give the title compound **17** (210 mg, yield 91%). mp 144−146 °C. ^{1}H NMR (DMSO-d_6, 500 MHz): δ 11.75 (1H, s), 8.58 (1H, s), 7.77 (1H, d, J = 2.5 Hz), 7.80 (1H, dd, J = 9.0, 2.5 Hz), 7.07 (1H, d, J = 9.0 Hz), 5.78 (2H, s), 4.01 (2H, t, J = 6.5 Hz), 2.58 (2H, q, J = 7.5 Hz), 2.47 (2H, q, J = 7.5 Hz), 1.74 (2H, m), 1.20 (3H, t, J = 7.5 Hz), 1.05 (3H, t, J = 7.5 Hz), 0.98 (3H, t, J = 7.5 Hz); ^{13}C NMR (DMSO-d_6, 125 MHz): δ 163.79, 161.99, 156.56, 153.00, 151.82, 134.38, 123.45, 122.62, 121.57, 120.16, 114.09, 70.78, 27.44, 22.52, 18.52, 13.88, 13.53, 10.93; LRMS m/z 345.3 [M + H]$^+$; HRMS (ESI) m/z calculated for $C_{18}H_{25}N_4O_3$ [M + H]$^+$ 345.1921, found 345.1921; HPLC purity 96.11%, t_r = 13.72 min.

***N*-(3-(5,6-Diethyl-4(3*H*)-pyrimidone-2-yl)-4-*n*-propoxyphenyl)-pyrrolyl-1-formamide (18).** The compound **8** (200 mg, 0.6 mmol) was dissolved in a mixture of dichloromethane (5 mL) and triethylamine (303 mg, 3 mmol), pyrrolidine-1-carbonyl chloride (133 mg, 1 mmol) was added at 0 °C, and the resulting mixture was stirred for 6 h. The reaction mixture was washed with water, and the organic phase was dried with anhydrous Na_2SO_4 and concentrated to give a residue, which was purified on a silica gel column to obtain **18** as an off white solid (170 mg, yield 70.8%). mp 126−127 °C.^{1}H NMR (CD_3OD, 500 MHz): δ 7.95 (1H, d, J = 2.0 Hz), 7.51 (1H, dd, J = 8.5, 2.0 Hz), 7.00 (1H, d, J = 8.5 Hz), 5.78 (2H, s), 4.02 (2H, t, J = 6.5 Hz), 3.36 (4H, m), 2.58 (2H, q, J = 7.5 Hz), 2.48 (2H, q, J = 7.5 Hz), 1.87 (4H, m), 1.79 (2H, m), 1.19 (3H, t, J = 7.5 Hz), 1.04 (3H, t, J = 7.5 Hz), 0.97 (3H, t, J = 7.5 Hz); ^{13}C NMR (CD_3OD, 125 MHz): δ 165.63, 163.06, 155.79, 153.21, 152.78, 133.12, 126.17, 123.37, 123.29, 120.01, 112.89, 70.78, 45.64, 27.15, 25.08, 22.12, 18.04, 12.36, 12.26, 9.55; LRMS m/z 399.3 [M + H]$^+$; HRMS (ESI) m/z calculated for $C_{22}H_{31}N_4O_3$ [M + H]$^+$ 399.2391, found 399.2398; HPLC purity 99.26%, t_r = 15.98 min.

***N*-(3-(5,6-Diethyl-4(3H)-pyrimidone-2-yl)-4-*n*-propoxyphenyl)oxalamide (19).** The compound **8** (337 mg, 1 mmol) was dissolved in dichloromethane (5 mL), and triethylamine (1 mL) was added, followed by slow addition of ethyl oxalyl monochloride (130 mg, 1 mmol) at 0 °C. After stirring for 0.5 h, the reaction mixture was washed with water (10 mL), 1 N HCl (5 mL), saturated sodium bicarbonate solution (10 mL), and saturated saline. The organic phase was dried with anhydrous Na_2SO_4 and concentrated under reduced pressure to obtain the residue, which was dissolved in a mixture of ammonia (0.5 mL) and methanol (4 mL) and stirred for 5 h. The reaction mixture was concentrated and purified using a silica gel column using ethyl acetate−petroleum ether as the eluent, to give the title compound as an off-white solid (240 mg, yield 64% over two steps). ^{1}H NMR (DMSO-d_6, 500 MHz): δ 11.80 (1H, s), 10.68 (1H, s), 8.31 (2H, s), 7.96 (2H, s), 7.89 (1H, dd, J = 9.0, 2.5 Hz), 7.17 (1H, d, J = 9.0 Hz), 4.05 (2H, t, J = 6.5 Hz), 2.58 (2H, q, J = 7.5 Hz), 2.46 (2H, q, J = 7.5 Hz), 1.76 (2H, m), 1.22 (3H, t, J = 7.5 Hz), 1.04 (3H, t, J = 7.5 Hz), 0.97 (3H, t, J = 7.5 Hz); ^{13}C NMR (DMSO-d_6, 125 MHz): δ 163.80, 162.81, 162.03, 159.17, 153.84, 152.79, 131.39, 130.12, 124.82, 123.60, 122.79, 113.73, 70.61, 27.39, 27.08, 22.57, 22.45, 18.51, 13.88, 13.53, 10.90; LRMS m/z 373.3 [M + H]$^+$; HRMS (ESI) m/z calculated for $C_{19}H_{25}N_4O_4$ [M + H]$^+$ 373.187, found 373.1877; HPLC purity 99.22%, t_r = 14.54 min.

***N*-(3-(5,6-Diethyl-4(3*H*)-pyrimidone-2-yl)-4-*n*-propoxyphenyl)-1-piperidineglyoxylamide (20).** The title compound was prepared in a similar manner to compound **19** using *N*-methylpiperazine instead of ammonia. Off-white solid (273 mg, yield 60% over two steps). mp 186−187 °C.^{1}H NMR ($CDCl_3$, 500 MHz): δ 11.15 (1H, s), 9.29 (1H, s), 8.42 (1H, d, J = 3.0 Hz), 7.98 (1H, dd, J = 9.0, 3.0 Hz), 7.02 (1H, d, J = 9.0 Hz), 4.31 (2H, m), 4.16 (2H, t, J = 6.5 Hz), 3.77 (2H, s), 2.68 (2H, q, J = 7.5 Hz), 2.60 (2H, q, J = 7.5 Hz), 2.53 (4H, m), 2.36 (3H, s), 1.98 (2H, m), 1.30 (3H, t, J = 7.5 Hz), 1.15 (6H, m); ^{13}C NMR ($CDCl_3$, 125 MHz): δ 164.53, 162.27, 160.09, 158.42, 154.48, 150.90, 130.81, 124.56, 124.49, 122.49, 119.90, 113.48, 71.47, 55.47, 54.66, 46.34, 45.84, 43.60, 27.68, 22.41, 18.73, 13.41, 13.18, 10.64; LRMS m/z 456.4 [M + H]$^+$; HRMS (ESI) m/z calculated for $C_{24}H_{34}N_5O_4$ [M + H]$^+$ 456.2605, found 456.2607; HPLC purity 98.99%, t_r = 15.07 min.

5,6-Diethyl-2-(2-*n*-propoxy-5-mesylamidophenyl)-4(3*H*)-pyrimidone (21). The compound **8** (337 mg, 1 mmol) was dissolved in dichloromethane (20 mL), and triethylamine (1 mL) was added, followed by slow addition of mesyl chloride (81 μL, 1 mmol) at 0 °C. After stirring for 0.5 h, the reaction mixture was washed with water (10 mL), 1 N HCl (5 mL), saturated sodium bicarbonate solution (10 mL), and saturated saline. The organic phase was dried with anhydrous Na_2SO_4 and concentrated under reduced pressure to obtain an oil, which was purified on a silica gel column using ethyl acetate−petroleum ether as an eluent, to give the title compound **21** as an off-white solid (360 mg, yield 95%). mp 140−141 °C. ^{1}H NMR ($CDCl_3$, 500 MHz): δ 8.29 (1H, d, J = 2.5 Hz), 7.51 (1H, dd, J = 9.0, 2.5 Hz), 7.31 (1H, s), 7.03 (1H, d, J = 9.0 Hz), 4.16 (2H, t, J = 7.0 Hz), 2.67 (2H, q, J = 7.5 Hz), 2.58 (2H, q, J = 7.5 Hz), 1.97 (2H, m), 1.29 (3H, t, J = 7.5 Hz), 1.14 (6H, m); ^{13}C NMR ($CDCl_3$, 125 MHz): δ 164.40, 162.73, 155.16, 150.98, 130.88, 127.12, 124.72, 124.39, 120.25, 113.91, 71.44, 39.18, 27.51, 22.34, 18.71, 13.39, 13.04, 10.59; LRMS m/z 380.3 [M + H]$^+$; HRMS (ESI) m/z calculated for $C_{18}H_{26}N_3O_4S$ [M + H]$^+$ 380.1639, found 380.1648; HPLC purity 98.50%, t_r = 19.02 min.

Protein Purification and Crystallization. The cDNA fragment-encoding catalytic domain of human PDE5A1 (residues 535−860) was cloned into the pET15b vector, and the protein was expressed in Rosetta2 (DE3) pLysS (Novagen). Purification of the PDE5A1 catalytic domain was based on the protocols reported previously. In brief, the lysate of expressed PDE5A1 was passed through a Ni-NTA column (Qiagen) and further purified with Q-Sepharose and Superdex200 (GE). The recombinant PDE5A1 with a purity of >95% was concentrated to 10 mg/mL for crystallization. Crystallization of apo PDE5A1 was performed at room temperature using the hanging drop vapor diffusion method, by mixing equal volumes of the protein and of the precipitant (19−20% (w/v) PEG 3350/200 mM $MgSO_4$/100 mM Tris−HCl at pH 7.5). Crystals formed within 5 days and were subsequently soaked in the crystallization solution with 1 mM **15** for 6 h. Then, the crystals were flash-frozen directly into liquid nitrogen with perfluoropolyether Cryo oil (Hampton Research) for cryoprotection.

Structure Determination and Refinement. X-ray diffraction data were collected at beamline BL18U1 at the Shanghai Synchrotron Radiation Facility (SSRF). The data were processed with HKL3000.[34] The structure was solved by molecular replacement by using the program CCP4 with a search model of PDB code 1T9R.[35,36] The model was built using COOT and refined with a simulated-annealing protocol implemented in the program PHENIX.[37,38] The relevant data collection and refinement statistics are given in Table 3.

PDE Enzyme Assay. The synthesized compounds were evaluated for their inhibitory activities against PDE5 as well as other PDEs through measurement of the hydrolysis of [^{3}H]-cGMP/[^{3}H]-cAMP into [^{3}H]-GMP/[^{3}H]-AMP using a phosphodiesterase scintillation proximity assay (SPA).[39] The enzymes were purchased from BPS Bioscience. The SPA beads, [^{3}H]-cGMP, and [^{3}H]-cAMP were purchased from PerkinElmer. The activity assays were performed

DOI: 10.1021/acs.jmedchem.9b00123
J. Med. Chem. 2019, 62, 4979−4990

according to the manufacturer's instructions. Assays were performed in the presence of 50 mM Tris−HCl (pH 7.5) containing 8.3 mM $MgCl_2$ and 1.7 mM EGTA. Each assay was performed in a 100 μL reaction volume containing the above buffer, enzyme, and around 0.05 μCi [^{3}H]-cGMP (for PDE5, PDE6, PDE9, and PDE11) or 0.05 μCi [^{3}H]-cAMP (for PDE1, PDE2, PDE3, PDE4, PDE7, PDE8, and PDE10). The reaction was carried out at 30 °C for 30 min and stopped by the addition of 50 μL PDE SPA beads (1 mg) suspended in 18 mM zinc sulfate. The reaction mixture was left to settle at room temperature for 20 min before counting using a MicroBeta TriLux (Perkin-Elmer Life Sciences, USA). Stock solutions of the compounds were prepared in 100% DMSO, diluted in deionized water to the appropriate concentrations, and added to the assay buffer to give a final concentration of <1% DMSO. The amount of enzyme used in each reaction was such that the hydrolysis of substrates did not exceed 15% so that the amount of product increased linearly with time. Each assay was run in triplicate. IC_{50} values were calculated from the concentration−inhibition curves by nonlinear regression analysis using GraphPad Prism.

Isothermal Titration Calorimetry (ITC). All experiments were performed with a Microcal ITC200 (GE) with a buffer containing 20 mM Tris at pH 7.5, 100 mM NaCl, 1 mM EDTA, 0.5 mM TCEP, and 5% glycerol while stirring at 800 rpm. Two inhibitors and the protein were diluted with the ITC buffer to a concentration of 200−250 and 20−25 μM, respectively, before titration. The final concentration of DMSO in the reaction buffer is less than 2% of the total volume. All titrations of inhibitors into PDE5A1 were performed using an initial injection of 0.4 μL followed by 19 identical injections of 2 μL with a duration of 4 s per injection and a spacing time of 150 s between injections. The last five data points were averaged and subtracted from each titration to account for the heat of dilution (inhibitor into protein). Additional background experiments where the buffer was titrated into the protein solution revealed no significant shift in the baseline during the course of the measurements.

HLM Metabolic Stability Test. Test compounds were dissolved in 100% DMSO to prepare a 10 mM stock solution and diluted to a final concentration of 1.0 μM for the experiments. The compound was incubated in a mix containing 0.5 mg/mL human liver microsome (HLM), 0.1 M phosphate buffer, and 1 mg/mL NADPH for 30 min and then the reaction was stopped by the addition of threefold volume of cold acetonitrile containing an internal standard. The incubation solution was centrifuged at 15,000 rpm for 5 min to precipitate proteins. An aliquot of 100 μL of the supernatant was used for LC/MS/MS analysis. Reaction without NADPH was used as a negative control to exclude the misleading factor that resulted from instability of the chemical itself. Midazolam was used as a positive control. Data are expressed as percent remaining after 30 min of incubation.

In Vivo Efficacy in the SHR Rat Model. All procedures performed on animals were in accordance with regulations and established guidelines and were reviewed and approved by the Institutional Animal Care and Use Committee at Shanghai Institute of Materia Medica, Chinese Academy of Sciences.

Male spontaneously hypertensive rats (SHRs) weighing 300−400 g purchased from Shanghai Slack Laboratory Animal Co., Ltd. were used in this test. After fasting for 12 h, six rats were randomized into each group. The test compounds dissolved in normal saline were administered to SHRs at a dose of 20 mg/kg by single gavage. Normal saline was used as a control. The heart rate and mean arterial blood pressure (mBP) were measured before and 0.5, 1, 2, 4, 6, and 24 h after drug administration using a noninvasive blood pressure monitoring system (Softron Biotechnology Ltd.). It was repeatedly measured three times at each time point.

In Vivo Efficacy in MCT-Induced PAH Rat Model. One hundred SD rats (5−6 weeks, 190−210 g) were purchased from Shanghai Sippr-BK laboratory animal Co. Ltd. (Shanghai, China). The rats were housed in a temperature- (20−26 °C) and moisture (RH: 40−70%)-controlled room exposed to a controlled 12 h cycle of light and darkness (light from 8:00 to 20:00), and allowed free access to food and water. All the rats were randomly allocated into five groups (each group, n = 20): control group (distillated water), model group (distillated water), sildenafil group (25 mg/kg), bosentan group (100 mg/kg), and **15** group (1 mg/kg). All the rats were injected subcutaneously with 60 mg/kg MCT (ethanol/normal saline = 2:8 as solvent), except the control group, which was injected subcutaneously with the same amount of solvent (ethanol/normal saline = 2:8 solution). **15**, sildenafil, and bosentan were dissolved in distillated water. Each group was given a corresponding dose of drug or distillated water after the MCT injection once a day for 21 days. Then, the right cardiac catheter method was applied to measure the pulmonary artery pressure, and the mean pulmonary artery pressure (mPAP) was used to conduct statistics.

Pharmacokinetics. Sprague−Dawley rats (three males and three females) weighing 180−220 g were purchased from Shanghai Sippr-BK laboratory animal Co. Ltd. (Shanghai, China). Beagle dogs (three males and three females) weighing 9−12 kg were purchased from Shanghai Jiaotong University Agriculture College Teaching Experiment Exercitation Plant (Shanghai, China). Compound **15** was administered orally and intravenously to rats and dogs after fasting for 12 h with free access to water. The dose for rats and dogs was 1.0 mg/kg and 0.5 mg/kg, respectively. Blood samples were collected at various time points during a 24 h period. Plasma concentrations of **15** were analyzed using an LC/MS/MS mothed.

■ ASSOCIATED CONTENT

Supporting Information

The Supporting Information is available free of charge on the ACS Publications website at DOI: 10.1021/acs.jmedchem.9b00123.

Molecular formula strings and some data (CSV)

Accession Codes

The atomic coordinates and structure factors have been deposited into the Protein Data Bank with an accession code of 6IWI. Authors will release the atomic coordinates and experimental data upon article publication.

■ AUTHOR INFORMATION

Corresponding Authors

*E-mail: hljiang@simm.ac.cn. Phone: +86-21-50805873 (H. J.).
*E-mail: ycxu@simm.ac.cn. Phone: +86-21-50801267 (Y. X.).
*E-mail: shenjingshan@simm.ac.cn. Phone: +86-21-20231962 (J. S.).

ORCID

Zhen Wang: 0000-0001-9450-2260
Zhijian Xu: 0000-0002-3063-8473
Weiliang Zhu: 0000-0001-6699-5299
Haji Akber Aisa: 0000-0003-4652-6879
Yechun Xu: 0000-0002-1581-6155
Jingshan Shen: 0000-0001-9679-9934

Author Contributions

#Z. W., X. J., and X. Z. contributed equally to this study. The manuscript was written through contributions of all authors. All authors have given approval to the final version of the manuscript.

Notes

The authors declare no competing financial interest.

■ ACKNOWLEDGMENTS

This study was supported by the Strategic Priority Research Program of Chinese Academy of Sciences (no. XDA12040103), the National Key R&D Program of China (no. 2016YFA0502301), the Scientific and Technological

DOI: 10.1021/acs.jmedchem.9b00123
J. Med. Chem. 2019, 62, 4979−4990

Innovation Program of Science and Technology Commission of Shanghai Municipality (no. 16431900600), the National Science & Technology Major Project "Key New Drug Creation and Manufacturing Program", China (no. 2018ZX09711002), and the National Natural Science Foundation of China (81422047).

■ ABBREVIATIONS

PDE5, cyclic nucleotide phosphodiesterase-5; PDEs, phosphodiesterases; cGMP, cyclic guanosine monophosphate; cAMP, cyclic adenosine monophosphate; t.i.d., ter in die; ED, erectile dysfunction; PAH, pulmonary arterial hypertension; ITC, isothermal titration calorimetry; HLM, human liver microsome; MCT, monocrotaline; SHR, spontaneously hypertensive rat; mBP, mean arterial blood pressure; mPAP, mean pulmonary artery pressure; C_{max}, the maximum plasma concentration; T_{max}, the time to reach C_{max}; AUC_{0-t}, total area under the plasma concentration−time curve from time zero to 24 h; $AUC_{0-\infty}$, total area under the plasma concentration−time curve from time zero to time infinity; MRT, mean retention time; $t_{1/2}$, terminal half-life; CL, plasma clearance; Vss, apparent volume of distribution at steady state; *F*, oral bioavailability

■ REFERENCES

(1) Sutendra, G.; Michelakis, E. D. Pulmonary arterial hypertension: challenges in translational research and a vision for change. *Sci. Transl. Med.* **2013**, *5*, 208sr5.
(2) Wilkins, M. R.; Aman, J.; Harbaum, L.; Ulrich, A.; Wharton, J.; Rhodes, C. J. Recent advances in pulmonary arterial hypertension. *F1000Research* **2018**, *7*, DOI: 10.12688/f1000research.14984.1.
(3) Schermuly, R. T.; Ghofrani, H. A.; Wilkins, M. R.; Grimminger, F. Mechanisms of disease: pulmonary arterial hypertension. *Nat. Rev. Cardiol.* **2011**, *8*, 443−455.
(4) Humbert, M.; Morrell, N. W.; Archer, S. L.; Stenmark, K. R.; MacLean, M. R.; Lang, I. M.; Christman, B. W.; Weir, E. K.; Eickelberg, O.; Voelkel, N. F.; Rabinovitch, M. Cellular and molecular pathobiology of pulmonary arterial hypertension. *J. Am. Coll. Cardiol.* **2004**, *43*, S13−S24.
(5) Wensel, R.; Opitz, C. F.; Anker, S. D.; Winkler, J.; Höffken, G.; Kleber, F. X.; Sharma, R.; Hummel, M.; Hetzer, R.; Ewert, R. Assessment of survival in patients with primary pulmonary hypertension: importance of cardiopulmonary exercise testing. *Circulation* **2002**, *106*, 319−324.
(6) Chun, K. J.; Kim, S. H.; An, B. J.; Kim, S. H.; Ha, J. K.; Hong, T. J.; Shin, Y. W. Survival and prognostic factors in patients with primary pulmonary hypertension. *Korean J. Intern. Med.* **2001**, *16*, 75−79.
(7) Ireland, R. Is PDE5 inhibition effective in pulmonary arterial hypertension? *Nat. Clin. Pract. Cardiovasc. Med.* **2006**, *3*, 63.
(8) Tantini, B.; Manes, A.; Fiumana, E.; Pignatti, C.; Guarnieri, C.; Zannoli, R.; Branzi, A.; Galié, N. Antiproliferative effect of sildenafil on human pulmonary artery smooth muscle cells. *Basic Res. Cardiol.* **2005**, *100*, 131−138.
(9) Stasch, J. P.; Evgenov, O. V. Soluble guanylate cyclase stimulators in pulmonary hypertension. *Handb. Exp. Pharmacol.* **2013**, *218*, 279−313.
(10) Safdar, Z. Treatment of pulmonary arterial hypertension: the role of prostacyclin and prostaglandin analogs. *Respir. Med.* **2011**, *105*, 818−827.
(11) Hamidi, S. A.; Lin, R. Z.; Szema, A. M.; Lyubsky, S.; Jiang, Y. P.; Said, S. I. VIP and endothelin receptor antagonist: an effective combination against experimental pulmonary arterial hypertension. *Respir. Res.* **2011**, *12*, 141.
(12) Ghofrani, H. A.; Osterloh, I. H.; Grimminger, F. Sildenafil: from angina to erectile dysfunction to pulmonary hypertension and beyond. *Nat. Rev. Drug Discovery* **2006**, *5*, 689−702.
(13) Daugan, A.; Grondin, P.; Ruault, C.; Le Monnier de Gouville, A.-C.; Coste, H.; Kirilovsky, J.; Hyafil, F.; Labaudinière, R. The discovery of tadalafil: a novel and highly selective PDE5 inhibitor. 1: 5,6,11,11a-tetrahydro-1H-imidazo[1′,5′:1,6]pyrido[3,4-b]indole-1,3(2H)-dione analogues. *J. Med. Chem.* **2003**, *46*, 4525−4532.
(14) Daugan, A.; Grondin, P.; Ruault, C.; Le Monnier de Gouville, A.-C.; Coste, H.; Linget, J. M.; Kirilovsky, J.; Hyafil, F.; Labaudinière, R. The discovery of tadalafil: a novel and highly selective PDE5 inhibitor. 2: 2,3,6,7,12,12a-hexahydropyrazino[1′,2′:1,6]pyrido[3,4-b]indole-1,4-dione analogues. *J. Med. Chem.* **2003**, *46*, 4533−4542.
(15) Abman, S. H.; Deruelle, P. NO-cGMP signaling in the pathogenesis and treatment of persistent pulmonary hypertension of the newborn. *BMC Pharmacol.* **2005**, *5*, S30.
(16) Wharton, J.; Strange, J. W.; Møller, G. M. O.; Growcott, E. J.; Ren, X.; Franklyn, A. P.; Phillips, S. C.; Wilkins, M. R. Antiproliferative effects of phosphodiesterase type 5 inhibition in human pulmonary artery cells. *Am. J. Respir. Crit. Care. Med.* **2005**, *172*, 105−113.
(17) Herschorn, S. Cardiovascular safety of PDE5 inhibitors. *Can. J. Urol.* **2003**, *10*, 23−28.
(18) Sandner, P.; Hütter, J.; Tinel, H.; Ziegelbauer, K.; Bischoff, E. PDE5 inhibitors beyond erectile dysfunction. *Int. J. Impotence. Res.* **2007**, *19*, 533−543.
(19) Lukowski, R.; Krieg, T.; Rybalkin, S. D.; Beavo, J.; Hofmann, F. Turning on cGMP-dependent pathways to treat cardiac dysfunctions: boom, bust, and beyond. *Trends Pharmacol. Sci.* **2014**, *35*, 404−413.
(20) Sitbon, O.; Gaine, S. Beyond a single pathway: combination therapy in pulmonary arterial hypertension. *Eur. Respir. Rev.* **2016**, *25*, 408−417.
(21) Wang, G.; Liu, Z.; Chen, T.; Wang, Z.; Yang, H.; Zheng, M.; Ren, J.; Tian, G.; Yang, X.; Li, L.; Li, J.; Suo, J.; Zhang, R.; Jiang, X.; Terrett, N. K.; Shen, J.; Xu, Y.; Jiang, H. Design, synthesis, and pharmacological evaluation of monocyclic pyrimidinones as novel inhibitors of PDE5. *J. Med. Chem.* **2012**, *55*, 10540−10550.
(22) Gong, X.; Wang, G.; Ren, J.; Liu, Z.; Wang, Z.; Chen, T.; Yang, X.; Jiang, X.; Shen, J.; Jiang, H.; Aisa, H. A.; Xu, Y.; Li, J. Exploration of the 5-bromopyrimidin-4(3H)-ones as potent inhibitors of PDE5. *Bioorg. Med. Chem. Lett.* **2013**, *23*, 4944−4947.
(23) Ren, J.; He, Y.; Chen, W.; Chen, T.; Wang, G.; Wang, Z.; Xu, Z.; Luo, X.; Zhu, W.; Jiang, H.; Shen, J.; Xu, Y. Thermodynamic and structural characterization of halogen bonding in protein-ligand interactions: a case study of PDE5 and its inhibitors. *J. Med. Chem.* **2014**, *57*, 3588−3593.
(24) Maurice, D. H.; Ke, H.; Ahmad, F.; Wang, Y.; Chung, J.; Manganiello, V. C. Advances in targeting cyclic nucleotide phosphodiesterases. *Nat. Rev. Drug Discov.* **2014**, *13*, 290−314.
(25) Bischoff, E. Potency, selectivity, and consequences of nonselectivity of PDE inhibition. *Int. J. Impotence. Res.* **2004**, *16*, S11−S14.
(26) Galiè, N.; Brundage, B. H.; Ghofrani, H. A.; Oudiz, R. J.; Simonneau, G.; Safdar, Z.; Shapiro, S.; White, R. J.; Chan, M.; Beardsworth, A.; Frumkin, L.; Barst, R. J. Tadalafil therapy for pulmonary arterial hypertension. *Circulation* **2009**, *119*, 2894−2903.
(27) Gbekor, E.; Betheil, S.; Fawcett, L.; Mount, N.; Phillips, S. Selectivity of sildenafil and other phosphodiesterase type 5 (PDE5) inhibitors against all human phosphodiesterase families. *Eur. Urol., Suppl.* **2002**, *1*, 63.
(28) Mirone, V.; Fusco, F.; Rossi, A.; Sicuteri, R.; Montorsi, F. Tadalafil and vardenafil vs sildenafil: a review of patient-preference studies. *BJU Int.* **2009**, *103*, 1212−1217.
(29) Seftel, A. D. Phosphodiesterase type 5 inhibitor differentiation based on selectivity, pharmacokinetic, and efficacy profiles. *Clin. Cardiol.* **2004**, *27*, I14−I19.
(30) Walker, D. K. Pharmacokinetics and metabolism of sildenafil in mouse, rat, rabbit, dog and man. *Xenobiotica* **2008**, *29*, 297−310.
(31) Wallace, A. C.; Laskowski, R. A.; Thornton, J. M. LIGPLOT: a program to generate schematic diagrams of protein-ligand interactions. *Protein Eng. Des. Sel.* **1995**, *8*, 127−134.

DOI: 10.1021/acs.jmedchem.9b00123
J. Med. Chem. 2019, 62, 4979−4990

(32) Schermuly, R. T.; Kreisselmeier, K. P.; Ghofrani, H. A.; Yilmaz, H.; Butrous, G.; Ermert, L.; Ermert, M.; Weissmann, N.; Rose, F.; Guenther, A.; Walmrath, D.; Seeger, W.; Grimminger, F. Chronic sildenafil treatment inhibits monocrotaline-induced pulmonary hypertension in rats. *Am. J. Respir. Crit. Care. Med.* **2004**, *169*, 39−45.
(33) Xu, Z.; Liu, Z.; Chen, T.; Chen, T.; Wang, Z.; Tian, G.; Shi, J.; Wang, X.; Lu, Y.; Yan, X.; Wang, G.; Jiang, H.; Chen, K.; Wang, S.; Xu, Y.; Shen, J.; Zhu, W. Utilization of halogen bond in lead optimization: a case study of rational design of potent phosphodiesterase type 5 (PDE5) inhibitors. *J. Med. Chem.* **2011**, *54*, 5607−5611.
(34) Minor, W.; Cymborowski, M.; Otwinowski, Z.; Chruszcz, M. HKL-3000: the integration of data reduction and structure solution–from diffraction images to an initial model in minutes. *Acta Cryst.* **2006**, *62*, 859−866.
(35) Collaborative, C. P. The CCP4 suite: programs for protein crystallography. *Acta Crystallogr., D: Biol. Crystallogr.* **1994**, *50*, 760−763.
(36) Zhang, K. Y. J.; Card, G. L.; Suzuki, Y.; Artis, D. R.; Fong, D.; Gillette, S.; Hsieh, D.; Neiman, J.; West, B. L.; Zhang, C.; Milburn, M. V.; Kim, S. H.; Schlessinger, J.; Bollag, G. A glutamine switch mechanism for nucleotide selectivity by phosphodiesterases. *Mol. Cell* **2004**, *15*, 279−286.
(37) Emsley, P.; Cowtan, K. Coot: model-building tools for molecular graphics. *Acta Crystallogr., D: Biol. Crystallogr.* **2004**, *60*, 2126−2132.
(38) Adams, P. D.; Grosse-Kunstleve, R. W.; Hung, L.-W.; Ioerger, T. R.; McCoy, A. J.; Moriarty, N. W.; Read, R. J.; Sacchettini, J. C.; Sauter, N. K.; Terwilliger, T. C. PHENIX: building new software for automated crystallographic structure determination. *Acta Cryst.* **2002**, *58*, 1948−1954.
(39) Khawaja, X.; Dunlop, J.; Kowal, D. Scintillation proximity assay in lead discovery. *Expert Opin. Drug Discovery* **2008**, *3*, 1267−1280.

DOI: 10.1021/acs.jmedchem.9b00123
J. Med. Chem. 2019, 62, 4979−4990